

Isotope effects in the kinetics of simultaneous H and D thermal desorption from Pd

F. Leardini*, J.F. Fernández, J. Bodega, C. Sánchez

Departamento de Física de Materiales, Universidad Autónoma de Madrid, 28049 Cantoblanco, Madrid, Spain

Received 16 May 2007; received in revised form 2 August 2007; accepted 10 August 2007

Abstract

The kinetics of simultaneous hydrogen and deuterium thermal desorption from PdH_xD_y has been investigated. A novel experimental approach for the study of the transition state (TS) characteristics of the surface recombination reaction is proposed based on the analysis of the H and D partitioning into H₂, HD and D₂ molecules. It has been found that the hydrogen molecular isotopes distribution is determined by the energy differences of the corresponding TS of the atom–atom recombination reactions. On the other hand, the mechanisms and activation energies of the desorption process have been obtained. At 420 K, the desorption reaction changes from a surface recombination limiting mechanism during desorption from β-PdH_xD_y to a reaction limited by the rate of β to α phase transformation during the two phase coexistence. Surface recombination reaction becomes again rate limiting above 480 K, due to a change in the catalytic properties of the Pd surface. TS energies obtained from the kinetic analysis of the thermal desorption spectra are in good accordance with those obtained from the analysis of the H₂, HD and D₂ distributions. Anomalous TS energies have been observed for the H–D recombination reaction, which may be related to the heteronuclear character of this molecule.

© 2007 Elsevier Ltd. All rights reserved.

PACS: 68.43.Mn; 68.43.Vx; 82.20.Db; 82.20.Pm; 82.20.Tr; 82.65.+r; 82.80.Ms

Keywords: A. Metals; C. Differential scanning calorimetry; D. Electrochemical properties; D. Thermodynamic properties

1. Introduction

Hydrogen is considered one of the main candidates to be the energy carrier in the near future. This fact has stimulated an important research activity on hydrogen storage methods. Hydrogen storage in metal hydrides (MH) appears to be a very suitable method [1]. One of the main issues in this field concerns the kinetics of hydrogen absorption/desorption. The formation/decomposition of a MH involves both bulk (hydride to solid solution phase transformations, diffusion of H atoms through the bulk and from the bulk to the surface) and surface (dissociation of H₂ molecules/H–H recombination at the surface) processes. In most cases, the H absorption/desorption kinetics in/from a MH is limited by surface reaction steps [2]. Accordingly, there is a growing interest on the catalysis

of surface reactions in MH [3,4]. In this context, the microscopic description of the MH formation/decomposition processes is of fundamental importance.

A suitable approach to investigate the kinetics of H atoms in the course of chemical reactions is the analysis of the H/D isotope effects. Owing to their relative mass differences, the hydrogen isotopes have different zero-point energies (ZPE) and local vibration modes within the wells of the potential energy surface (PES). As a consequence of these energy shifts, the reaction rates are usually higher for the lighter isotope. This is denoted as the normal isotope effect. However, there are some exceptions to this rule. A typical case is the inverse isotope effect observed in the H/D diffusion in Pd [5].

H/D isotope effects appear in very different conditions and phenomena. The simplest reaction involving H and D atoms is the isotope exchange reaction:



*Corresponding author. Tel.: +34914974777; fax: +34914978579.
E-mail address: fabrice.lear dini@uam.es (F. Leardini).

Reaction (1) has been proved to be very useful to investigate the kinetics and mechanisms of the interaction of H_2 with metal surfaces. This reaction has been extensively investigated on mono- and polycrystalline transition metal surfaces [6–14] as well as on transition metal supported catalysts [15–18]. H/D kinetic isotope effects in hydride forming metals have been also widely investigated, mainly due to the potential applications of MH for isotope separation processes. This kind of studies is usually performed by heterophase hydrogen isotope exchange (H_2/MD and D_2/MH) experiments [19,20].

In the present work, the kinetics of simultaneous hydrogen and deuterium desorption from bulk PdH_xD_y material is investigated by means of thermal desorption spectroscopy (TDS). TDS was initially developed for the study of the desorption kinetics of chemical species from surfaces, but lately it has been proved to be also a valuable technique to investigate the kinetics of MH decomposition [21–23]. Two relevant facts support the election of Pd hydride to perform this investigation. Firstly, the Pd/ H_2 system is the prototypic MH system. Historically, it was the first MH that attracted research activities [24] and it has been the most investigated MH since then. Secondly, Pd is well known for its selectivity and activity in hydrogenation reactions and it is one of the most used catalysts. Indeed, Pd thin film overlayers are usually used to enhance the kinetics of hydrogen uptake and release from MH [25,26].

Isotope effects in the kinetics of H(D) absorption/desorption by/from α -Pd and α -Pd–Pt alloys have been recently reported [27,28]. These studies show the existence of an inverse isotope effect in the kinetics of α -Pd decomposition. Nevertheless, to our knowledge, isotope effects in the kinetics of PdH_xD_y decomposition (within the hydride region) have not been investigated yet. Moreover, there is only one previous TDS study on the simultaneous H and D desorption from MH [29]. This investigation was carried out in V and V–Ti intermetallic compounds, although no quantitative analysis of the desorption kinetics was reported in that paper.

A novel experimental approach for the study of the transition state (TS) characteristics of the surface recombination reaction is proposed here based on the analysis of the H and D distribution into H_2 , HD and D_2 molecules. This technique can give complementary information to that obtained on TS from quantum-state resolved experiments [30] and quantum-state integral measurements [14].

2. Experimental

Pd foils (Goodfellow, 99.95%) have been simultaneously hydrogenated–deuterated by electrolysis in 0.1 M LiOH–LiOD electrolyte at room temperature (RT). The original thicknesses of the foils were 0.25 mm and the geometrical area in contact with the electrolyte 0.57 cm^2 . The foils were washed in an ultrasound bath with ethanol and then with deionised water ($18.6\text{ M}\Omega\text{ cm}$) prior to the electrolytic experiments. The electrolyte was prepared by

dissolving metallic granulated lithium in a mixture of H_2O ($18.6\text{ M}\Omega\text{ cm}$) and D_2O ($>99.6\%$ isotopic purity, $0.08\text{ M}\Omega\text{ cm}$) under Ar atmosphere. The H/D ratio in the electrolyte was 0.22 ± 0.01 . The electrolysis was performed with a Princeton Mod.362 potentiostat in a three-electrode open cell all constructed in Teflon. Pd foils were placed at the bottom of the electrolytic cell with only one face in contact with the electrolyte. Counter electrode was a Pt grid located opposite to the cathode and the reference electrode was a Pt wire placed near the cathode. Several charge/discharge cycles were applied to the sample before the experiments by accomplishing voltammograms between -0.2 and -3 V at a sweep rate of 0.02 V s^{-1} . Then, Pd electrodes were charged at constant electrode potential, $E_{Pd/Pt} = -3\text{ V}$, until hydrogen–deuterium evolution was observed. Finally, the electrolytic current was reversed by applying an electrode potential equal to -0.2 V . The charge through the electrodes during this oxidation stage was below 1% of that passed during the cathodic polarization of the electrodes. After the electrolytic H and D charging, the foils were handled in air to perform the structural, morphological and electrical characterization.

Structural characterization of the samples at RT has been carried out by means of X-ray diffraction (XRD) accomplished with the CuK_α radiation in a θ – 2θ Siemens D-5000 powder diffractometer. Sample surface morphology and composition have been studied with a Phillips XL30 scanning electron microscope (SEM) equipped with electron dispersive X-ray (EDAX) analysis.

Electrical resistivity measurements have been done by Van der Pauw method [31] with a Keithley Mod. 2400 current source and a Keithley Mod.182 digital voltmeter. Thermopower measurements have been performed as described elsewhere [32].

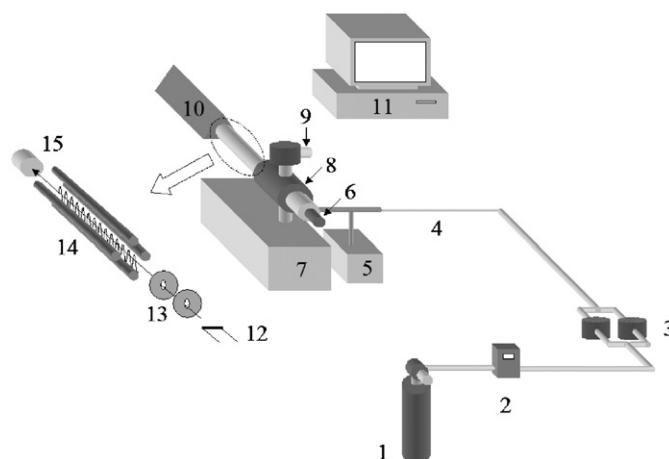


Fig. 1. Scheme of the experimental system used for TDS measurements: (1) Ar bottle; (2) flow meter and controller; (3) differential scanning calorimeter; (4) capillary tube; (5) rotary pump; (6) dosing valve; (7) turbomolecular pump; (8) vacuum chamber; (9) Penning sensor; (10) electronic setup; (11) PC acquisition data and controller system; (12) ion source; (13) electrodes; (14) quadrupolar filter; (15) ion detector.

TDS has been performed in the experimental setup depicted in Fig. 1. A differential scanning calorimeter (Perkin-Elmer DSC4) is connected through a quartz capillary tube and a dosing valve (Balzers UDV 040) to a quadrupole mass spectrometer (QMS 200 Balzers) placed inside a high vacuum chamber. A more detailed description of the experimental system can be found in [23].

A constant Ar flow (57.6 sccm, 99.999% purity) passing symmetrically through both heaters of the calorimeter was used to carry the desorbed gases to the QMS. Thermal desorption spectra have been obtained by heating the samples between 298 and 623 K at a constant heating rate equal to 0.333 K s^{-1} . Mass of the samples before and after TDS experiments were measured with a balance Ohaus Analytical Plus.

The current intensity and energy of the ionizing electrons in the QMS were 2 mA and 100 eV, respectively. Detailed calibrations of the gas analysis system have been performed prior to TDS experiments [33]. At the experimental conditions of the present TDS experiments, the i_2 , i_3 and i_4 current peaks are essentially due to H_2^+ , HD^+ and D_2^+ ions, respectively (the contribution of D^+ , H_3^+ and H_2D^+ ions to these current peaks were below 1%). In addition, the influence of isotope exchange reactions among the hydrogen ionic/molecular isotopes during the gas analysis process has been found to be negligible. Therefore, the H_2 , HD and D_2 desorbed flows (f_χ) are related to the i_2 , i_3 and i_4 peak currents, respectively, according to

$$i_{m/q}(\chi) - i_{m/q}^0(\chi) = \sigma_{m/q}(\chi)f_\chi, \quad (2)$$

where $i_{m/q}^0$ represent the background signals from the residual atmosphere present in the vacuum chamber and $\sigma_{m/q}(\chi)$ is the detection sensitivity of the specie χ . The obtained detection sensitivities for H_2 , HD and D_2 gases are equal to 1.62×10^{-4} , 6.25×10^{-5} and $3.74 \times 10^{-5} \text{ A mol}^{-1} \text{ s}$, respectively, to within $\pm 3\%$. The observed differences among the detection sensitivities of the hydrogen molecular isotopes come from the mass discrimination effects in the gas collection, pumping and ion filtering processes [33]. Experimental base lines have been recorded before the TDS experiments to obtain the temperature dependence of the $i_{m/q}^0$ peak currents.

3. Results

3.1. Characterization of PdH_xD_y samples

Pd cathodes have been characterized by means of XRD, electrical resistivity and thermopower measurements after the electrolytic H/D charging in order to know the amount of H and D atoms present in PdH_xD_y . Three Pd foils charged with different H and D concentrations have been investigated. The results derived from the kinetic analysis of the TDS curves are reproducible to within 5%. Here, only the results obtained from one of the samples will be presented for the sake of clarity.

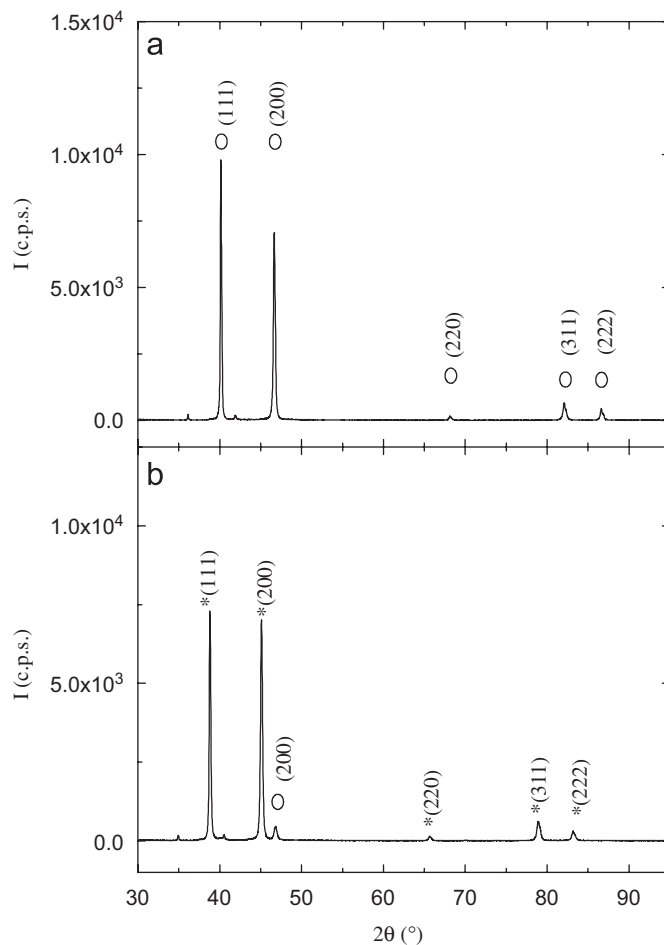


Fig. 2. XRD patterns of Pd sample before (a) and after (b) electrochemical hydrogenation–deuteration. Diffraction peaks of α -Pd and β -Pd hydride–deuteride are labelled with open circles and stars, respectively. Diffracting planes corresponding to each XRD peak are indexed. Non-labelled peaks correspond to diffraction produced by residual Cu $K\alpha$ radiation.

Table 1
Lattice parameters, resistivity and Seebeck coefficients of Pd and β - PdH_xD_y at RT

	Pd		β - PdH_xD_y		
	This work	Literature	This work	$\text{PdH}_{0.6}$	$\text{PdD}_{0.6}$
a (Å)	3.892(3)	3.89019 [34]	4.022(3)	4.025[35]	4.025 [36]
ρ ($\mu\Omega \text{ cm}^{-1}$)	9.9(1)	10.54 [37]	18.5(2)	17.9 [38]	20.0 [38]
S_c ($\mu\text{V K}^{-1}$)	-11.0(1)	-11.5 [39]	5.1(1)	5 [39]	

The XRD patterns of Pd before and after electrochemical hydrogenation are shown in Fig. 2(a) and (b), respectively. These patterns can be indexed in the $Fm\bar{3}m$ crystallographic space group, characteristic of Pd and β -Pd hydride–deuteride. Diffraction peaks of Pd and β -Pd H_xD_y have been labelled with open circles and stars, respectively. Diffracting planes corresponding to each XRD peak have been indexed. Non-labelled small peaks correspond to the diffraction produced by non-filtered $\text{CuK}\beta$ radiation.

The lattice parameters of Pd and β -PdH_xD_y obtained from the analysis of the XRD patterns are summarized in Table 1, together with the results reported by other authors. A good agreement is observed between the present experimental values and those obtained in previous works. This coincidence and the practical absence of diffraction peaks corresponding to α -Pd in the XRD pattern of PdH_xD_y (only a weak diffraction peak from the (200) plane of α -Pd is observed) reflect that the sample composition is close to the limit of the α - β transition, β_{\min} . At RT this limit corresponds to a content of 0.61 H+D atoms per Pd atom [35]. This value, together with the x/y ratio determined by integration of the QMS signals during TDS (see Section 3.2) gives $x = 0.35 \pm 0.01$ and $y = 0.26 \pm 0.01$.

The measured resistivities of the Pd and PdH_xD_y samples are shown in Table 1, together with the values reported for Pd [37], PdH_{0.6} [38] and PdD_{0.6} [38] materials. It can be seen that there is a relatively large isotope effect that affects the resistivities of Pd hydride and deuteride. By considering that the electrical resistivity of β -Pd(H-D)_{0.6} depends linearly on the relative H and D content, the electrical resistivity of PdH_{0.35}D_{0.26} would be $18.7 \mu\Omega \text{ cm}^{-1}$. This value agrees with the present experimental result and confirms the calculation of the H and D concentration in the Pd matrix.

The measured Seebeck coefficients of Pd and PdH_xD_y (Table 1) are close to the values reported for Pd and PdH_{0.6} [39]. As far as we know, no data on the Seebeck coefficient of Pd deuteride have been previously reported. The present result on the Seebeck coefficient of PdH_{0.35}D_{0.26} implies that there are not large differences between the Seebeck coefficients of Pd hydride and deuteride.

The obtained x and y ratios are also consistent with the electrolytic separation factor (S) between the atoms contained in the hydride and in the electrolyte. For hydride forming electrodes, S is defined as

$$S = \frac{(H/D)_{\text{liq}}}{(H/D)_{\text{M}}}, \quad (3)$$

where $(H/D)_{\text{M}}$ and $(H/D)_{\text{liq}}$ refer to the fractions of H and D in the metal hydride and in the electrolyte, respectively. S is determined by the difference in the absorption rates of H and D atoms by Pd during the electrolysis [33]. From the measurements of the H and D fractions in the PdH_xD_y sample and in the electrolyte, a S value equal to 6.2 ± 0.6 is obtained, which is quite close to those reported by Farkas [40] ($S = 6.6$) and Dandapani and Fleischmann [41] ($S \sim 7.2$).

Lattice parameter, resistivity and Seebeck coefficient measurements indicate a total (H+D) content close to β_{\min} (0.61), what is in good agreement with the value obtained from the integration of the TDS peaks and from the mass loss measurements of the sample before and after TDS. The mass of the PdH_xD_y sample was 13.34 ± 0.01 mg and the mass loss after the desorption 0.12 ± 0.02 mg. These data give $x+y = 0.67 \pm 0.15$. The large error in the $x+y$

value comes from the 16% of error in the mass loss measurement and the 6% of error in the x/y ratio.

The morphology and composition of the Pd foils have been investigated by SEM–EDAX analysis. No remarkable differences have been observed in the cathode surface before and after electrolytic hydrogenation–deuteration.

3.2. Thermal desorption spectra of PdH_{0.35}D_{0.26}

TDS of the PdH_{0.35}D_{0.26} foil is shown in Fig. 3a. This spectra consists of a single desorption peak for each one of the hydrogen molecular isotopes. The H₂, HD and D₂ flows have been normalized to their maximum values in order to clarify the comparison among them. Absolute values of H₂, HD and D₂ flows at the maxima of TDS peaks are 6.72×10^{-8} , 9.61×10^{-8} and $3.09 \times 10^{-8} \text{ mol s}^{-1}$, respectively.

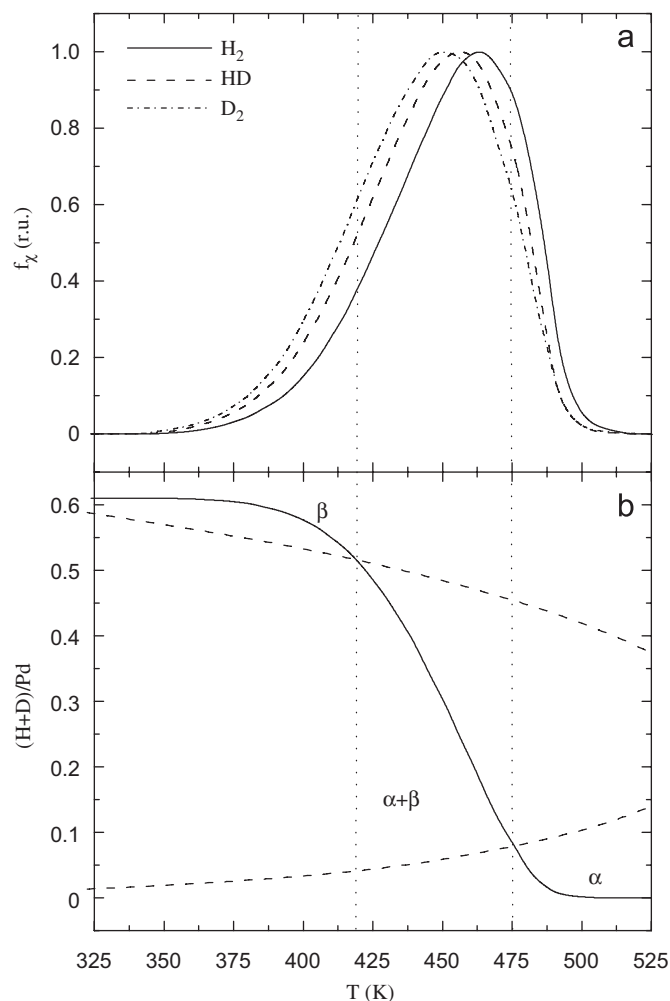


Fig. 3. (a) Normalized H₂, HD and D₂ flows desorbed from PdH_xD_y as a function of temperature during a linear temperature ramp (0.333 K s^{-1}); (b) H plus D fraction remaining in the sample as a function of temperature. This fraction has been obtained by integration of TDS curves. Dashed lines show the temperature dependence of the two phase coexistence limits [31]. Vertical dotted lines show the temperatures at which the H+D concentration crosses the limits of the β -PdH_xD_y and α -Pd phases.

An inverse isotope effect is observed. The desorption peak is shifted to higher temperatures for H₂ than for D₂, being the HD peak between the H₂ and D₂ ones. The temperatures at which the maxima of the peaks occur are 448.5, 458.3 and 461.9 K for D₂, HD and H₂, respectively. It should be noted that these temperature shifts are not due to the time required for the transport of the desorbed molecules from the sample surface to the gas analysis system. In fact, the observed shifts are opposite to what would be observed if they were caused by the transport of gases because the diffusion of the heavier molecule towards the QMS is slower. Besides, the experimental system has been constructed to reduce the transport time as much as possible and it has been estimated to be <10 s [23].

The TDS peaks for the three hydrogen molecular isotopes are asymmetric, with a sharper fall of the desorbed flows at temperatures higher than that corresponding to their maxima. A detailed examination reveals that this fall is sharper for HD than for H₂ and D₂. Similar H₂ desorption peaks have been reported from TDS of β-PdH_x powder [42] and β-PdH_x foils [43] formed by solid–gas reactions and from thermogravimetric analysis of electrochemically loaded PdH_x foils [44].

An *x/y* ratio equal to 1.37 ± 0.08 in PdH_xD_y has been obtained after integration of the H₂, HD and D₂ desorption peaks. Error comes mainly from the uncertainty in the determination of the detection sensitivities $\sigma_{m/q}(\chi)$. Besides, the integration of the TDS curves allows the obtaining of the temperature variation of the H plus D fraction in Pd, as shown in Fig. 3b. The two phase coexistence limits [35] are also plotted in Fig. 3b (dashed lines), in order to emphasize the temperatures at which the total H plus D concentration crosses the limits of the β-PdH_xD_y and α-Pd phases, namely 420 and 475 K, respectively. The small H/D isotope effects in the limits of the β-PdH_xD_y and α-Pd phases [45] have been neglected.

4. Discussion

4.1. Partitioning of H and D atoms into H₂, HD and D₂ molecules

The desorbed H₂, HD and D₂ molecules are formed at the sample surface by recombination of H and D atoms. Therefore, the way in which H and D surface atoms are partitioned into the three molecular isotopes must depend on the characteristics of these reactions. Owing to ZPE differences, significant isotope effects are expected among the kinetics of the H–H, H–D and D–D recombination reactions. However, earlier kinetic studies on the isotope exchange reaction (1) on metal surfaces have usually assumed no isotope effects in the rates of H and D recombination reactions [9–13], in order to simplify the theoretical analysis. This assumption implies a statistical partitioning of H and D atoms into H₂, HD and D₂ molecules. In other works [19], the relative concentrations of the hydrogen molecular isotopes in the gas phase have

been assumed to be determined by the equilibrium constant of reaction (1):

$$K_{\text{eq}} = \frac{[\text{HD}]^2}{[\text{H}_2][\text{D}_2]}, \quad (4)$$

The statistical value of K_{eq} for equally probable combination of H and D atoms is 4. However, a lower value is found in practice due to the fact that a pair of H₂ and D₂ molecules is energetically more favourable than two of HD. Exact calculations of K_{eq} were made by Urey and Rittenberg [46] based on the partition functions of the molecules. In the temperature range of the present TDS experiments their results can be approximated by

$$\ln K_{\text{eq}} = \frac{-6.75 \times 10^{-3}}{kT} + 1.4471, \quad (5)$$

where k is the Boltzmann constant expressed in eV K⁻¹.

The integration of the H₂, HD and D₂ flows desorbed from PdH_{0.35}D_{0.26} yields a ratio among the three molecular isotopes of ~2:3:1. Those ratios disagree with the expected ones either from statistical or equilibrium partitioning of H and D atoms into H₂, HD and D₂ molecules. A detailed examination of the relative amounts of H₂, HD and D₂ desorbed molecules reported in previous experimental works also reveals deviations from statistical or equilibrium partitioning among the molecules [11,19,47,48]. In particular, experimental results on hydrogen–deuterium exchange on Pd [19] showed departures from the equilibrium value predicted by Eq. (5), although equilibrium was later assumed to simplify the theoretical analysis. It is worth to note, however, that experimental values of the relative amounts of H₂, HD and D₂ molecules are not given in most of the previous works [6–10,12–18].

It will be shown here that the assumptions of equilibrium or statistical partitioning of H and D atoms into the three molecular isotopes are only valid under certain circumstances. We will deal with the general case in which H₂, HD and D₂ molecules are formed by surface recombination of H and D atoms. Two limiting cases must be distinguished:

- (i) Surface recombination reaction is at equilibrium (i.e., takes place in the forward and backward directions).
- (ii) Surface recombination is out of equilibrium (i.e., takes place in the forward direction only).

In the first case, the molecules are continuously dissociated and formed at the surface and, therefore, equilibrium partitioning of H and D atoms into hydrogen molecules is expected. However, in the majority of the experiments involving H and D atoms to form H₂, HD and D₂ molecules by surface recombination (such as TDS), the molecules are rapidly removed from sample surface by means of a pumping system or a carrier gas flow. Under these circumstances it is reasonable to assume that surface recombination reaction occurs in the forward direction only (i.e., case (ii) holds), whichever be the rate-determining step of the whole reaction. Accordingly, the H₂, HD

and D₂ desorbed flows (f_{HH} , f_{HD} and f_{DD} , respectively) can be written as

$$f_{HH} = v_{HH} \exp\left(-\frac{E_{HH}^* - 2E_H^p}{kT}\right) \theta_H^2, \quad (6a)$$

$$f_{HD} = v_{HD} \exp\left(-\frac{E_{HD}^* - E_H^p - E_D^p}{kT}\right) \theta_H \theta_D, \quad (6b)$$

$$f_{DD} = v_{DD} \exp\left(-\frac{E_{DD}^* - 2E_D^p}{kT}\right) \theta_D^2, \quad (6c)$$

where v_{HH} , v_{HD} and v_{DD} are the preexponential factors of the H–H, H–D and D–D recombination processes; E_{HH}^* , E_{HD}^* and E_{DD}^* are the corresponding energy levels of the transition states; E_H^p and E_D^p are the energy levels of H and D atoms at the precursor (surface) states of molecular formation and θ_H and θ_D are their respective concentrations.

In order to quantify the relationship among the H₂, HD and D₂ desorbed flows let us to define, in analogy with Eq. (4):

$$K = \frac{f_{HD}^2}{f_{HH}f_{DD}}. \quad (7)$$

Introducing Eqs. (6a)–(6c) into (7) and taking logarithms, it is obtained:

$$\ln K = \ln \left[\frac{v_{HD}^2}{v_{HH}v_{DD}} \right] - \frac{2E_{HD}^* - E_{HH}^* - E_{DD}^*}{kT}. \quad (8)$$

In the absence of isotope effects in the atom–atom recombination reaction, $v_{HD} = 2v_{HH} = 2v_{DD}$ and $E_{HH}^* = E_{HD}^* = E_{DD}^*$, what implies a statistical partitioning of atoms into the molecular isotopes (i.e., $K = 4$). However, we believe that this assumption is unrealistic because large ZPE differences among H–H, H–D and D–D pairs at the TS are expected.

Experimental TDS data of PdH_{0.35}D_{0.26} have been analyzed according to Eq. (8) and the results are shown in Fig. 4. The line predicted by the equilibrium exchange reaction (5) is also plotted (dashed line) for comparison purposes. Experimental points in Fig. 4 show two regions (A and B) that can be fitted by Eq. (8). According to the present model, this behaviour denotes a change in the energy levels of the TS of the atom–atom recombination. This change occurs at ~480 K and it is quite abrupt. The temperature range where the transition takes place is of about 10 K. The least square fits of experimental points in Fig. 4 (solid lines) give energies of -0.051 ± 0.001 and -0.96 ± 0.07 eV in regions A and B, respectively. The appearance of negative energies simply reflects that the TS energy of the H–D recombination is below the mean value between H–H and D–D ones. This finding contrasts with the predictions of simple quantum considerations, as it will be shown in Section 4.3.

It is worth to emphasize that although the rates of H₂, HD and D₂ desorption may depend on other steps of the whole process, the relationship among these flows defined

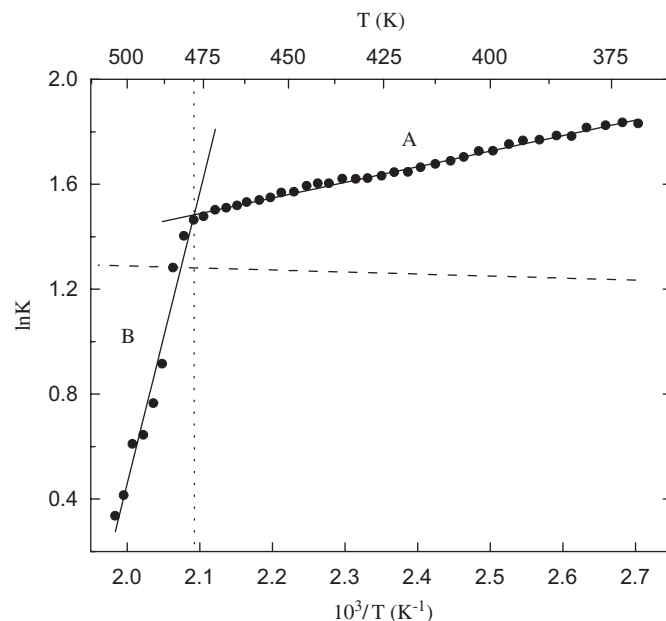


Fig. 4. Arrhenius plot of the relative H₂, HD and D₂ flows desorbed from PdH_xD_y (black points). Two regions appear with different activation energies denoted as A and B in the figure. The vertical dotted line shows the temperature at which the change from region A to B occurs (~480 K). Solid lines represent the linear fit to the data in both regions. The line predicted by the equilibrium exchange reaction between H₂ and D₂, Eq. (5), has been also plotted (dashed line) for comparison purposes.

by (7) is uniquely determined by the atom–atom recombination reaction, according to Eq. (8). Therefore, the logarithmic plot in Fig. 4 can be taken as a direct insight into the TS of the surface recombination reaction.

4.2. Kinetic analysis of the thermal desorption spectra

In order to analyze the kinetics of the thermal desorption process, one should consider the desorption mechanism which can be summarized in up to six sequential steps:

- Diffusion of H and D atoms through β -PdH_xD_y.
- Transformation of β -PdH_xD_y into α -Pd.
- Diffusion of H and D atoms through α -Pd.
- Transition of H and D atoms from bulk to surface states.
- Surface recombination of H and D atoms to form H₂, HD and D₂ physisorbed molecules.
- Desorption of physisorbed molecules into the gas phase.

It should be noted that these steps are not simultaneously present during the complete desorption reaction. According to Fig. 3b, the total H and D concentration crosses the limits of the β -PdH_xD_y and α -Pd phases. During desorption from β -PdH_xD_y steps (b) and (c) are absent, whereas the same occurs with steps (a) and (b) during desorption from α -Pd. Therefore, one should analyze separately the desorption kinetics depending on the steps involved in each region.

It must be pointed out here that only the values of the activation energies of the desorption process will be obtained from such analysis. The frequency factors appearing in the kinetic equations cannot be obtained from the present experimental data because there are some unknown variables in these equations, such as the geometrical factors ‘ M ’.

4.2.1. Desorption from β -PdH_xD_y

Below 420 K, the PdH_xD_y sample is in the β -phase (see Fig. 3b). The H and D concentration gradients within the sample in this temperature region are small and, therefore, diffusion does not control the desorption process. These gradients can be evaluated from the ratios $\Delta x/x$ and $\Delta y/y$, where Δx and Δy are the variations of the H and D concentrations inside the sample during a typical diffusion time τ [42]:

$$\Delta x = f_H \tau_H, \quad (9a)$$

$$\Delta y = f_D \tau_D, \quad (9b)$$

where f_H and f_D are the H and D desorption rates. On the other hand, τ can be estimated according to $\tau = L^2/\pi^2 D_c$, where L is the diffusion length and D_c is the diffusion coefficient of H or D ($D_c = D_0 \exp(-E_d/kT)$). We have used a diffusion length of one-half of the Pd foil thickness. Therefore, Δx and Δy should be considered as an estimation of the H and D concentration gradients between the centre and the surfaces of the Pd foil.

The diffusion coefficient of H in β -Pd hydride is given by $D_0 = 0.9 \times 10^{-3} \text{ cm}^2 \text{ s}^{-1}$ and $E_d = 0.228 \text{ eV}$ [49]. Deuterium diffusion coefficients have been calculated from reported data [50] of the ratio between H and D diffusion coefficients in Pd as a function of temperature. The obtained $\Delta x/x$ and $\Delta y/y$ values at 400 K are equal to 0.013 and 0.014, respectively. From those results it is clear that the desorption process cannot be fitted by a diffusion limited mechanism.

The analysis of the thermal desorption curves of bulk MH in the case of a process limited by surface recombination was done by Stern et al. [21,22] and was successfully applied to Pd hydride powder [42]. They considered two limiting cases, depending on the relative position of the H energy levels in the bulk and at the precursor (surface) states of the recombination reaction. According to their results, for a H/Pd ratio in the sample below 0.7, the H bonding energy in the bulk is higher than at the precursor states. Under these circumstances the H concentration at the precursor states is low and the H₂ flow can be written as

$$f_{\text{HH}} = M_s^A v_{\text{HH}}^A \exp\left(-\frac{E_{\text{HH}}^A - 2\mu_{\text{H}}}{kT}\right), \quad (10)$$

where M_s^A is a constant, v_{HH}^A is the frequency factor of H–H recombination and μ_{H} is the chemical potential of H atoms in the hydride. By writing analogue expressions for HD and D₂ flows and taking the chemical potential of H

and D atoms given by lattice gas theory [22], it is obtained:

$$f_{\text{HH}} = M_s^A v_{\text{HH}}^A \exp\left(-\frac{E_{\text{HH}}^A - 2E_{\text{H}}^\beta}{kT}\right) \left(\frac{x}{1-x}\right)^2, \quad (11a)$$

$$f_{\text{HD}} = M_s^A v_{\text{HD}}^A \exp\left(-\frac{E_{\text{HD}}^A - E_{\text{H}}^\beta - E_{\text{D}}^\beta}{kT}\right) \left(\frac{x}{1-x}\right) \left(\frac{y}{1-y}\right), \quad (11b)$$

$$f_{\text{DD}} = M_s^A v_{\text{DD}}^A \exp\left(-\frac{E_{\text{DD}}^A - 2E_{\text{D}}^\beta}{kT}\right) \left(\frac{y}{1-y}\right)^2, \quad (11c)$$

where E_{H}^β and E_{D}^β are the energies of H and D atoms, respectively, in bulk β -PdH_xD_y sites. The superscript A in the TS energies of the atom–atom recombination reaction denotes that this is the TS corresponding to region A in Fig. 4.

The H₂, HD and D₂ flows desorbed from β -PdH_xD_y have been fitted by Eqs. (11a)–(11c) and the results are shown in Fig. 5. Activation energies equal to 0.878 ± 0.004 , 0.822 ± 0.004 and $0.818 \pm 0.003 \text{ eV mole}^{-1}$ for H₂, HD and D₂, respectively, have been obtained from the least square fit of experimental points in this figure. The activation energies decrease in the order H₂ > HD > D₂, as expected from the temperature shift of H₂, HD and D₂ desorption peaks (Fig. 3a). This result is somewhat similar to that found by Jin et al. [27,28], who reported an inverse isotope effect in the kinetics of H(D) desorption from α -Pd. On the other hand, these activation energies imply the existence of an activation barrier for the surface recombination reaction, because they are higher than the formation

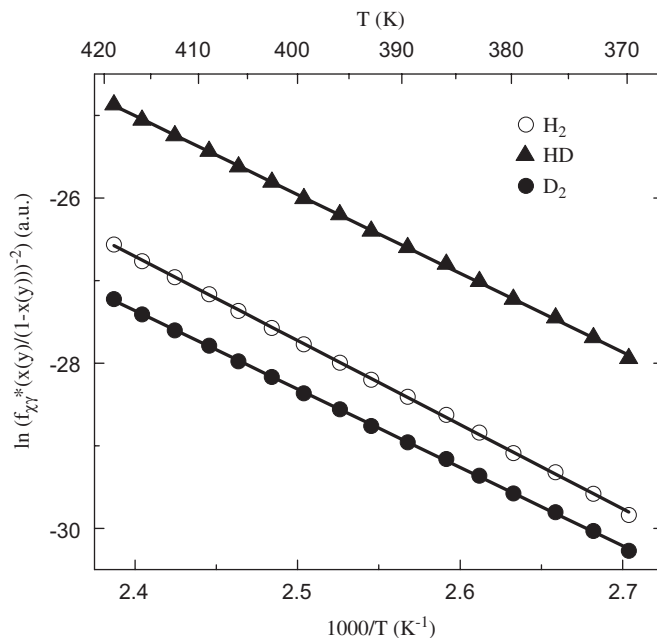


Fig. 5. Arrhenius plot of the H₂, HD and D₂ desorption by considering a surface recombination mechanism ($T < 420 \text{ K}$). Solid lines in this figure are the linear fits of experimental data.

enthalpies of β -Pd hydride and deuteride [45]. These barriers are higher than those obtained by Stern et al. [42]. Such differences should be attributed to the different surface conditions of the Pd samples. In fact, the height of the activation barrier for recombinative desorption is extremely sensitive to the presence of oxides [51,52] and other surface impurities [28,29,53].

4.2.2. Desorption during coexistence of the α and β phases

According to the model described in the previous section, if surface recombination is still rate limiting during the coexistence of β -PdH_xD_y and α -Pd, the molecular desorbed flows should be described by zero-order processes [42]. This is because the constancy of the H and D chemical potentials during the two-phase coexistence. However, the experimental H₂, HD and D₂ desorbed flows do not fit to a zero-order process.

The role of bulk diffusion has been analyzed as described above. In this case, diffusion coefficients in both β -PdH_xD_y and α -Pd phases have been used. Diffusion coefficients are faster in α -Pd than in β -PdH_xD_y. According to Völk and Alefeld [50] the best fit to diffusion coefficient data of H in α -Pd is given by $D_0 = 2.9 \times 10^{-3} \text{ cm}^2 \text{ s}^{-1}$ and $E_d = 0.230 \text{ eV}$. Again, D diffusion coefficients in α -Pd have been calculated from the reported ratio between H and D diffusion coefficients [50]. By using α and β diffusion coefficients, the lower and higher limits, respectively, for $\Delta x/x$ and $\Delta y/y$ can be estimated. The obtained values at 455 K are $0.02 < \Delta x/x, \Delta y/y < 0.07$. These concentration gradients imply that the kinetics of H and D desorption in this region is not controlled by diffusion.

Accordingly, there is only one possible mechanism to explain the desorption kinetics during the two-phase coexistence region, i.e., the transition of H and D atoms from the β -PdH_xD_y to the α -Pd phase. In this case, the rates of H and D desorption can be written as

$$f_H = M_{\beta} v_H \exp\left(-\frac{E_H^{\beta/\alpha} - E_H^{\beta}}{kT}\right) x_{\beta/\alpha}, \quad (12a)$$

$$f_D = M_{\beta} v_D \exp\left(-\frac{E_D^{\beta/\alpha} - E_D^{\beta}}{kT}\right) y_{\beta/\alpha}, \quad (12b)$$

where M_{β} is a constant, v_H and v_D are the frequency factors of the β to α transformation, $E_H^{\beta/\alpha}$ and $E_D^{\beta/\alpha}$ are the corresponding TS energies for H and D atoms and $x_{\beta/\alpha}$ and $y_{\beta/\alpha}$ are the numbers of H and D atoms at the β/α interface. These numbers will depend on the β -phase concentration (β_{\min} , which depends on temperature according to the dashed line shown in Fig. 3b) and on the area of the β/α interface ($A_{\beta/\alpha}$):

$$x_{\beta/\alpha} = c \frac{x}{x+y} \beta_{\min} A_{\beta/\alpha}, \quad (13a)$$

$$y_{\beta/\alpha} = c \frac{y}{x+y} \beta_{\min} A_{\beta/\alpha}, \quad (13b)$$

where c is a constant. The factors $x/(x+y)$ and $y/(x+y)$ account for the probability of a H or D atom be located at the β/α interface, respectively.

In this model, the desorbing sample must be regarded as a shrinking core of β -PdH_xD_y enveloped by a growing layer of α -Pd [54]. Due to the fact that the hydrogen and deuterium partial pressures in the volume near the sample are much lower than the equilibrium pressures of the β/α transformation, the H and D concentration in α -Pd can be safely assumed to be negligible. This implies that all the remaining H and D atoms are in the β -PdH_xD_y inner core. Accordingly, the volume of this core should be proportional to the total number of atoms in the sample $(x+y)$, while the area of the β/α interface should be proportional to $(x+y)^{2/3}$. Taking into account those considerations, Eqs. (12a) and (12b) take the form:

$$f_H = M'_{\beta} v_H \exp\left(-\frac{E_H^{\beta/\alpha} - E_H^{\beta}}{kT}\right) \beta_{\min} x (x+y)^{-1/3}, \quad (14a)$$

$$f_D = M'_{\beta} v_D \exp\left(-\frac{E_D^{\beta/\alpha} - E_D^{\beta}}{kT}\right) \beta_{\min} y (x+y)^{-1/3}. \quad (14b)$$

The experimental H and D desorbed flows have been fitted by Eqs. (14a) and (14b), respectively, and the results are shown in Fig. 6. According to the present model, H and D atoms desorb from the β -PdH_xD_y inner core and, therefore, the β to α phase transformation should control the process until the end of the desorption process. However, it can be seen from Fig. 6 that the model only fit the experimental data up to $\sim 480 \text{ K}$. This is the temperature at which the change from region A to region

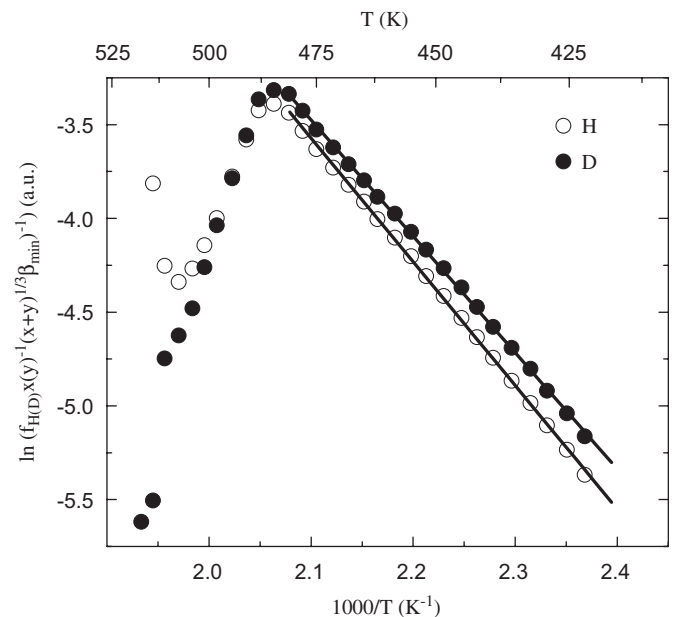


Fig. 6. Arrhenius plot of the H and D flows by considering a β to α transformation mechanism ($420 < T < 480 \text{ K}$). Solid lines in this figure are the linear fits of experimental data.

B is observed in the plot of the relative desorbed flows (Fig. 4), which was ascribed to a change in the kinetics of the surface recombination reaction.

Activation energies equal to 0.569 ± 0.003 and 0.535 ± 0.003 eV atom⁻¹ for H and D, respectively, have been obtained from the slopes of the least square fits of the experimental points in Fig. 6. These values imply the existence of an inverse isotope effect in the β to α transition. As far as we know, no previous results on this isotope effect have been reported. In addition, there is only one previous estimation of the activation energy of the β to α transition in the Pd–D system [55]. It was obtained from the analysis of the effective diffusion coefficient of D in single crystal Pd within the two-phase coexistence region. The reported activation energy value was 0.45 eV atom⁻¹, which is in reasonable agreement with the present result.

4.2.3. Final stage of desorption

As it has been stated in the previous section, above 480 K the desorption kinetics is not controlled by the β to α phase transition. This has been ascribed to the change in the kinetics of the surface recombination reaction, which becomes again rate limiting above this temperature. This implies that the rate of the β to α phase transition is now faster than the whole desorption rate. Given that the mean H plus D concentration in the sample in this temperature range is below the α -Pd phase limit (see Fig. 3b), it is expected that the inner β -nucleus will disappear and the sample will be completely transformed into α -Pd.

Again, the role of bulk diffusion on the desorption process has been estimated. Diffusion coefficients in α -Pd have been used. At 495 K, the obtained $\Delta x/x$ and $\Delta y/y$ ratios are equal to 0.07 and 0.06, respectively.

Following the analysis done in Section 4.2.1 for a surface recombination limiting mechanism, the H₂, HD and D₂ flows will be described by the following equations:

$$f_{\text{HH}} = M_s^{\text{B}} v_{\text{HH}}^{\text{B}} \exp\left(-\frac{E_{\text{HH}}^{\text{B}*} - 2E_{\text{H}}^{\alpha}}{kT}\right) \left(\frac{x}{1-x}\right)^2, \quad (15a)$$

$$f_{\text{HD}} = M_s^{\text{B}} v_{\text{HD}}^{\text{B}} \exp\left(-\frac{E_{\text{HD}}^{\text{B}*} - E_{\text{H}}^{\alpha} - E_{\text{D}}^{\alpha}}{kT}\right) \left(\frac{x}{1-x}\right) \left(\frac{y}{1-y}\right), \quad (15b)$$

$$f_{\text{DD}} = M_s^{\text{B}} v_{\text{DD}}^{\text{B}} \exp\left(-\frac{E_{\text{DD}}^{\text{B}*} - 2E_{\text{D}}^{\alpha}}{kT}\right) \left(\frac{y}{1-y}\right)^2, \quad (15c)$$

where M_s^{B} is a constant, v_{HH}^{B} , v_{HD}^{B} and v_{DD}^{B} are the frequency factors of the H–H, H–D and D–D recombination in region B (see Fig. 4) and E_{H}^{α} and E_{D}^{α} are the energies of H and D atoms, respectively, in α -Pd sites.

The fits of the experimental data by Eqs. (15a)–(15c) are shown in Fig. 7. The obtained activation energies are equal to 4.20 ± 0.06 , 3.65 ± 0.02 and 4.08 ± 0.05 eV mole c⁻¹ for H₂, HD and D₂, respectively. Those values are about five times greater than these found for the atom-atom

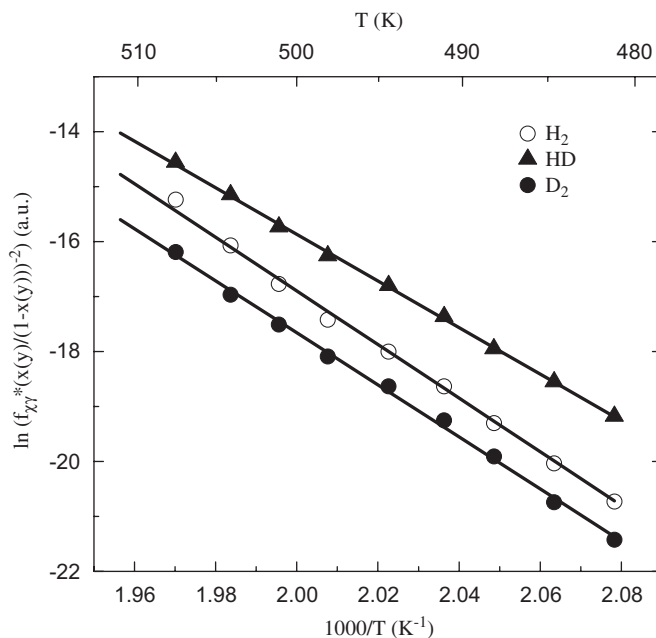


Fig. 7. Arrhenius plot of the H₂, HD and D₂ desorption by considering a surface recombination mechanism ($T > 480$ K). Solid lines in this figure are the linear fits of experimental data.

recombination in β -PdH_xD_y (Section 4.2.1). Similar increments in the activation energies of the atom–atom recombination have been observed in TDS experiments of TaD_x foils [56]. In these experiments, the surface composition was *in situ* monitored by means of Auger spectroscopy. The change of the activation energy occurred at the same temperature where a decrease in the oxygen surface concentration was observed. The authors argued that the increment in the activation energy of the H–H recombination reaction was due to the energy involved in the process of diffusion of oxygen atoms from the surface layer to the bulk.

Later experiments [57] performed in ultrahigh vacuum conditions with TaH_x and ZrH_x foils with different degrees of oxidation confirmed the observation of a rise in the activation energy of the H–H surface recombination. In this case, however, the effect was ascribed to the energy involved in the O desorption in the form of H₂O molecules.

The H₂O/HDO/D₂O desorption rates could not be monitored in our TDS experiments, due to a secondary effect that masked these signals. This effect consists on the hydrogen-induced water formation in the gas analysis chamber. Indeed, the H₂O/H₂ ratio in the present TDS experiments was similar to that observed during calibration experiments with H₂–Ar mixtures (typically in the range of 10⁻³–10⁻²). This ratio is in agreement with the previous investigations on the H₂-induced H₂O production [58,59]. Accordingly, the H₂O/HDO/D₂O signals coming from the H₂/HD/D₂-induced reactions within the QMS were much higher than those expected from the H₂O/HDO/D₂O desorption from the sample. This last quantity is several orders of magnitude lower than the H₂/HD/D₂ desorbed

flows. Even if one assumes that all the oxygen atoms present as impurities in the carrier Ar flow, whose concentration is <1 ppm, react with the desorbing H and D atoms at the Pd surface to form water molecules, the estimated $\text{H}_2\text{O}/\text{H}_2$ ratio would be about one order of magnitude lower than the measured one.

In any case, neither O diffusion into the bulk nor $\text{H}_2\text{O}/\text{HDO}/\text{D}_2\text{O}$ desorption can account for the present results. Within these models, the change of the activation energy of the desorption process is due to the extra energy needed either to diffuse O atoms into the bulk or to desorb them as $\text{H}_2\text{O}/\text{HDO}/\text{D}_2\text{O}$ molecules. Both processes would lead to a similar increment in the activation energies of H_2 , HD and D_2 molecules. By contrast, it is observed that the activation energy increments are different for the three hydrogen molecular isotopes. We hypothesize that the increment of the activation energies of the H–H, H–D and D–D recombination reactions should be attributed to a change of the surface catalytic properties due a modification of the surface composition. This modification would shift the energy levels of the TS's of the surface recombination reaction, which are different for each one of the molecular isotopes. This interpretation is further supported by the fact that the change in the activation energies occurs in the same temperature range than the change in the TS energies deduced from the analysis of the relative H_2 , HD and D_2 distributions (Fig. 4). This point will be considered in more detail in the next section. On the other hand, the modification of the surface composition should be ascribed to the diffusion of bulk impurities to the surface or to the growing of the surface oxide layer. Oxygen transitions from surface to subsurface or bulk sites have been reported in Pd [60] at temperatures between ~ 350 and 500 K. This would imply that the oxide layer present at the sample surface could growth, assisted by the oxygen diffusion into the bulk, due to the impurity levels of oxygen in the carrier Ar gas (~ 1 ppm). Further experiments must be accomplished to test the proposed model.

4.3. Transition state energies

The schematic diagram appearing in Fig. 8 shapes the energy levels of H and D atoms during the desorption reaction. The zero-energy level has been taken as the energy of a pair of free H atoms. The energy levels of H_2 , HD and D_2 molecules in the gas phase (E_{HH}^0 , E_{HD}^0 and E_{DD}^0) have been calculated from the reported dissociation energies of the three molecular isotopes [61]. It must be noted that dissociation energies refer to H_2 , HD and D_2 dissociation into atoms in their fundamental states. Therefore, the energy difference between free H and D atoms (3.6×10^{-3} eV) must be taken into account in the calculation of H_2 , HD and D_2 energies. The energy of H atoms in bulk α -Pd sites (E_{H}^{α}) has been obtained from E_{HH}^0 and the enthalpy of solution of H_2 in α -Pd. [35]. From E_{H}^{α} and the reported ZPE difference between H and D atoms in α -Pd [45], E_{D}^{α} can be calculated. On the other hand, H and D

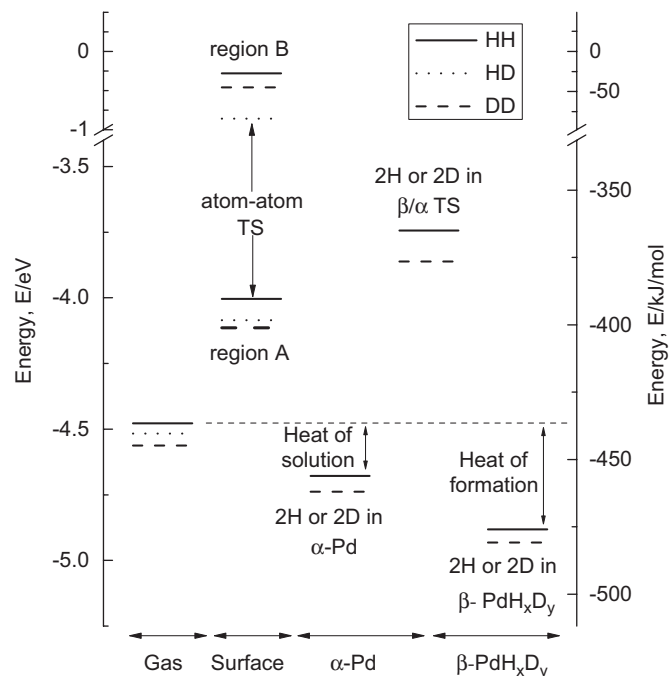


Fig. 8. Schematic diagram for the energy levels of H and D atoms in their desorption from PdH_xD_y .

energies in bulk β - PdH_xD_y sites (E_{H}^{β} and E_{D}^{β}) can be obtained from the enthalpies of the β to α transition of Pd hydride and deuteride [45], respectively. The energies of H and D atoms at the TS's of the β to α phase transformation and of the atom-atom surface recombination have been calculated from E_{H}^{α} , E_{D}^{α} , E_{H}^{β} , E_{D}^{β} and the activation energies obtained in the analysis of the TDS curves (Section 4.2).

The observed isotope effect in the TS energies (Fig. 8) can be understood in the following terms. The TS is usually represented as a saddle point at the PES, with a maximum along the reaction coordinate and a minimum in at least one of the normal coordinates. The dynamics of atoms or molecules along these normal coordinates generates quantized energy levels at the TS, which will depend on the mass of the atoms/molecules. The existence of such quantized states in the TS of chemical reactions is supported by some experimental evidences and it has been the subject of recent reviews [62,63]. TS energies of the β to α transition shown in Fig. 8 are more positive for H than for D atoms, as expected from the ZPE differences. Moreover, these differences are higher at the TS of the β to α transition than in bulk β - PdH_xD_y sites. This is the cause of the inverse isotope effect in the activation energies of the β to α phase transformation. A similar situation is observed for the TS of H and D diffusion in α -Pd. Differences between ZPE of H and D atoms are higher at the TS of the diffusion process than in α -Pd octahedral sites, which is the reason to observe a higher diffusion coefficient for D than for H [5,64].

Concerning the TS of the H–H, H–D and D–D surface recombination reactions, it is worth to note that when TS energies in Fig. 8 are introduced into Eq. (8), the values

obtained from the linear fit of the experimental points in Fig. 4 are reproduced within the experimental error. This accordance confirms the goodness of the calculation of the TS energies and, therefore, corroborates the kinetic analysis of the TDS curves.

On the other hand, the energy spacing among the H–H, H–D and D–D TS shows an anomalous behaviour. Considering the simplest case of a two-dimensional PES in which the potential along the normal coordinate is harmonic, the relative ZPE differences at the TS of H–H, H–D and D–D recombination can be calculated. Applying the rule for calculating isotopic energy levels [65], the difference between ZPE of H–H and H–D TS should be ~ 0.45 times the difference between H–H and D–D. This implies that ZPE of H–D TS should lie slightly above the mean value between H–H and D–D ones. This picture describes well the differences between ZPE of H₂, HD and D₂ molecules in the gas phase. However, as it can be seen in Fig. 8, H–D TS energies lay below the mean values of H–H and D–D TS energies. The effect is more pronounced in region B, in which TS energy of H–D is even lower than the corresponding value for D–D.

Anomalous behaviours among H₂, HD and D₂ molecules desorbed from Pd have been also observed by Schröter et al. [66]. They found that the energy spacing between the two first vibrational levels in the TS of the atom-atom recombination does not scale with the isotopic mass ratio of the molecules. Assuming that the energy difference between vibrational states is proportional to ZPE, as in the case of a harmonic potential, the ratio between the ZPE differences for the three molecular isotopes can be obtained from the experimental results of Schröter et al. [66]. It is found that ZPE of H–D recombination lies also below the mean value between H–H and D–D ones.

Tentative explanations of the above mentioned anomalies can be given on the basis of the heteronuclear character of the HD molecule. This gives rise to the breakdown of the inversion symmetry and to the appearance of several properties qualitatively different from those of the homonuclear species. A review of the phenomena associated to the inversion symmetry breakdown in HD has been recently done by de Lange et al. [67]. One of such phenomena is the existence of a permanent dipolar moment in the ground state of the HD molecule. This implies that TS energy of HD could be lowered by the presence of a surface electric field. However, by considering a typical electric field of 10^7 V m^{-1} , the dipolar moment of the HD molecule in the TS should be 6–7 orders of magnitude greater than the corresponding value in the fundamental state in the gas phase ($\sim 10^{-3} \text{ D}$ [68]) if the observed energy shifts are to be explained. Such a value seems to be unreasonable. On the other hand, the breaking of the inversion symmetry also produces the electronic coupling between states of *g* and *u* symmetry and this can lead to the appearance of new states not observed in the homonuclear species. This effect is stronger near the

dissociation threshold of the molecule [67]. The fact that the anomalies observed in the TS energies are more pronounced in region B, for which the TS energy is closer to the free atoms state, could be related to the former view. The present results motivate further experiments in order to clarify the origin of these anomalies, such as quantum-state integral measurements (i.e., the analysis of the angular and velocity distributions) and quantum state resolved experiments (i.e., the analysis of the rotational and vibrational distributions) of the desorbed molecular isotopes.

5. Conclusions

The kinetics of simultaneous hydrogen and deuterium desorption from PdH_xD_y has been investigated by means of TDS.

On the one hand, the H and D partitioning into the H₂, HD and D₂ desorbed molecules has been analyzed. It has been found that this partitioning is determined by the differences among the TS energies of the H–H, H–D and D–D recombination reactions. This finding contrasts with previous investigations that assumed either equilibrium or statistical partitioning of H₂, HD and D₂ molecules. The analysis of the relative concentration of the hydrogen molecular isotopes allows to follow the position of the H–D TS energy with respect to the mean value between the H–H and D–D ones during the course of the desorption reaction. As a consequence, the influence of the surface properties on the atom-atom recombination reaction can be easily monitored from the analysis of the H₂, HD and D₂ distributions.

The kinetics and mechanisms of the PdH_xD_y desorption have been derived from the analysis of the TDS curves. During desorption from the β -PdH_xD_y phase ($T < 420 \text{ K}$), a surface recombination mechanism (with activation energies equal to 0.878 ± 0.004 , 0.822 ± 0.004 and $0.818 \pm 0.003 \text{ eV mole}^{-1}$ for H₂, HD and D₂, respectively) has been observed. The desorption reaction has been found to be rate limited by the rate of the β to α phase transformation during the two-phase coexistence region, with activation energies equal to 0.569 ± 0.003 and $0.535 \pm 0.003 \text{ eV atom}^{-1}$ for H and D, respectively. Finally, surface recombination becomes again rate limiting above $\sim 480 \text{ K}$ due to a change in the surface activation barrier of the atom-atom recombination. This produces an increase of a factor ~ 5 in the activation energies of the atom-atom recombination (4.20 ± 0.06 , 3.65 ± 0.02 and $4.08 \pm 0.05 \text{ eV mole}^{-1}$ for H₂, HD and D₂, respectively).

TS energies of the β to α phase transformation and of the atom-atom recombination reaction have been calculated. TS energies for the H–D surface recombination have been found to be below the arithmetical mean value between the H–H and D–D TS energies. This fact contrasts with the predictions of simple quantum considerations. Tentative explanations related to the heteronuclear character of the

HD molecule have been proposed to explain the observed anomalies.

Acknowledgements

This work has been supported by Spanish MEC under contracts MAT2004-01903 and MAT2005-06738-C02-01. One of us (FL) also thanks to the Spanish MEC for a Ph.D. fellowship under the FPU program. Technical assistance from Mr. F Moreno is gratefully acknowledged. Finally, we want to thank one of the reviewers for several useful suggestions, mainly for his/her contribution to Fig. 8.

References

- [1] L. Schlapbach, A. Züttel, *Nature* 414 (2001) 353.
- [2] L. Schlapbach, in: L. Schlapbach (Ed.), *Hydrogen in Intermetallic Compounds*, vol. II, Springer, Berlin, 1992 Ch.2.
- [3] A. Borgschulte, R.J. Westervaal, J.H. Rector, H. Schreuders, B. Dam, R. Griessen, *J. Catal.* 239 (2006) 263.
- [4] K.S. Jung, D.H. Kim, E.Y. Lee, K.S. Lee, *Catal. Today* 120 (2007) 270.
- [5] G. Sicking, *J. Less Common Met.* 101 (1984) 169.
- [6] K.E. Lu, R.R. Rye, *Surf. Sci.* 45 (1974) 677.
- [7] S.L. Bernasek, G.A. Somorjai, *J. Chem. Phys.* 62 (1975) 3149.
- [8] I.E. Wachs, R.J. Madix, *Surf. Sci.* 58 (1976) 590.
- [9] M. Salmerón, R.J. Gale, G.A. Somorjai, *J. Chem. Phys.* 70 (1979) 2807.
- [10] T. Engel, H. Kuipers, *Surf. Sci.* 90 (1979) 162.
- [11] St.J. Dixon-Warren, A.T. Pasteur, D.A. King, *J. Chem. Phys.* 103 (1995) 2261.
- [12] M.F. Bertino, J.P. Toennies, *J. Chem. Phys.* 110 (1999) 9186.
- [13] P. Hahn, M.F. Bertino, J.P. Toennies, M. Ritter, W. Weiss, *Surf. Sci.* 412/413 (1998) 82.
- [14] T.H. Lin, G.A. Somorjai, *J. Chem. Phys.* 81 (1984) 704.
- [15] J. Magnusson, *Ind. Eng. Chem. Res.* 26 (1987) 877.
- [16] H. Backman, J. Jensen, F. Klingstedt, J. Wärna, T. Salmi, D.Y. Murzin, *Appl. Catal. A* 273 (2004) 303.
- [17] M.G. Basallote, S. Bernal, J.M. Gatica, M. Pozo, *Appl. Catal. A* 232 (2002) 39.
- [18] H. Backman, K. Rahkamaa-Tolonen, J. Wärna, T. Salmi, D.Y. Murzin, *Chem. Eng. J.* 107 (2005) 89.
- [19] G.W. Foltz, C.F. Melius, *J. Catal.* 108 (1987) 409.
- [20] D.A. Outka, G.W. Foltz, *J. Catal.* 130 (1991) 268.
- [21] A. Stern, S.R. Kreitzman, A. Resnik, D. Shaltiel, V. Zevin, *Solid State Commun.* 40 (1981) 837.
- [22] A. Stern, A. Resnik, D. Shaltiel, *J. Less Comm. Met.* 88 (1982) 431.
- [23] J.F. Fernández, F. Cuevas, C. Sánchez, *J. Alloys Compds.* 298 (2000) 244.
- [24] T. Graham, *Phil. Trans. Roy. Soc. (London)* 156 (1866) 415.
- [25] M.A. Pick, J.W. Davenport, M. Strongin, G.J. Dienes, *Phys. Rev. Lett.* 43 (1979) 286.
- [26] F. Cuevas, M. Hirscher, *J. Alloys Compds.* 313 (2000) 269.
- [27] Y. Jin, M. Hara, J.L. Wan, M. Matsuyama, K. Watanabe, *J. Alloys Compds.* 340 (2002) 207.
- [28] Y. Jin, L. Wang, M. Hara, K. Watanabe, *Mater. Trans.* 48 (2007) 560.
- [29] S. Hayashi, *J. Alloys Compds.* 359 (2003) 281.
- [30] L. Schöter, H. Zacharias, R. David, *Phys. Rev. Lett.* 62 (1989) 571.
- [31] L.J. Van der Pauw, *Phil. Res. Rep.* 13 (1958) 1.
- [32] J.R. Ares, M. Leon, N.M. Arozamena, J. Sánchez-Paramo, P. Celis, I.J. Ferrer, C. Sánchez, *J. Phys.: Condens. Matter* 10 (1998) 4281.
- [33] F. Leardini, J. Bodega, J.F. Fernández, I.J. Ferrer, C. Sánchez, *Recent Res. Dev. Electrochem.* 8 (2005) 257 (Kerala: Transworld Research Network).
- [34] A. Kern, W. Eysel, *Mineralogisch-Petrograph, Inst., Univ. Heidelberg, Germany, ICDD Grant-in-Aid*, 1993.
- [35] E. Wicke, H. Brodowski, in: G. Alefeld, J. Völk (Eds.), *'Hydrogen in Metals II' Topics in Applied Physics*, vol. 29, Springer, Berlin, 1978, pp. 73–155.
- [36] R. Felici, L. Bertalot, A. DeNinno, A. LaBarbera, V. Violante, *Rev. Sci. Instrum.* 66 (1995) 3344.
- [37] *CRC Handbook of Chemistry and Physics*, 82nd ed., ed Lide DR, CRC Press, Boca Raton, 2001–2002
- [38] M.C.H. McKubre, S. Crouch-Baker, M. Riley, R.C. Rocha-Filho, M. Schreiber, S.I. Smedley, F.L. Tanzella, Aspects of the electrochemical loading of hydrogen and its isotopes into palladium, in: Presented at ECS Meeting, Phoenix, Arizona, 1991
- [39] C.L. Foiles, *Solid State Commun.* 33 (1980) 125.
- [40] A. Farkas, *Trans. Farad. Soc.* 33 (1937) 552.
- [41] B. Dandapani, M. Fleischmann, *J. Electroanal. Chem.* 39 (1972) 323.
- [42] A. Stern, A. Resnik, D. Shaltiel, *J. Phys. F.: Met. Phys.* 14 (1984) 1625.
- [43] A.L. Cabrera, E. Morales, J.N. Amor, *J. Mater. Res.* 10 (1995) 779.
- [44] L.E.A. Berlouis, P.J. Hall, A.J. MacKinnon, A.W. Wark, D. Manuelli, V. Gervais, J.E. Robertson, *J. Alloys Compds.* 253/254 (1997) 207.
- [45] R. Läser, K.H. Klatt, *Phys. Rev. B* 28 (1983) 748.
- [46] H.C. Urey, D. Rittenberg, *J. Chem. Phys.* 1 (1933) 137.
- [47] Z. Liu, L.C. Feldmann, L.H. Tolc, Z. Zhang, P.I. Cohen, *Science* 312 (2006) 1024.
- [48] P. Franzen, R. Behrisch, C. García-Rosales, D. Schlessner, D. Rösler, J. Becker, W. Knapp, C. Edelmann, *Nucl. Fusion* 37 (1997) 1375.
- [49] E.F.W. Seymour, R.M. Cotts, W.D. Williams, *Phys. Rev. Lett.* 35 (1975) 165.
- [50] J. Völk, G. Alefeld, in: G. Alefeld, J. Völk (Eds.), *'Hydrogen in Metals I' Topics in Applied Physics*, vol. 28, Springer, Berlin, 1978, pp. 321–348.
- [51] G. Krenn, C. Eibl, W. Mauritsch, E.L.D. Hebenstreit, P. Varga, A. Winkler, *Surf. Sci.* 445 (2000) 343.
- [52] L.-G. Petersson, H. Dannetum, J. Fogelberg, I. Lundström, *Appl. Surf. Sci.* 27 (1986) 275.
- [53] F.J. Castro, G. Meyer, G. Zampieri, *J. Alloys compds.* 330–332 (2002) 612.
- [54] F.J. Castro, G. Meyer, *J. Alloys Compds.* 330–332 (2002) 59.
- [55] W.C. Chen, B.J. Heuser, *J. Alloys Compds.* 312 (2000) 59.
- [56] E. Pörschke, D. Shaltiel, K.H. Klatt, H. Wenzl, *J. Phys. Chem. Solids* 47 (1986) 1003.
- [57] D.E. Shleifman, D. Shaltiel, I.T. Steinberger, *J. Alloys Compds.* 223 (1995) 81.
- [58] H.F. Dylla, W.R. Blanchard, *J. Vac. Sci. Technol. A* 1 (1983) 1297.
- [59] J.R.J. Bennett, R.J. Elsey, *Vacuum* 44 (1993) 647.
- [60] J.-W. He, U. Memmert, P.R. Norton, *J. Chem. Phys.* 90 (1989) 5088.
- [61] G. Herzberg, *Phys. Rev. Lett.* 23 (1969) 1081.
- [62] K. Liu, *Annu. Rev. Phys. Chem.* 52 (2001) 139.
- [63] R.T. Skodje, X. Yang, *Int. Rev. Phys. Chem.* 23 (2004) 253.
- [64] X. Ke, G.J. Kramer, *Phys. Rev. B* 66 (2002) 184304.
- [65] G. Herzberg, *Molecular Spectra and Molecular Structure I. Spectra of Diatomic Molecules*, Nostrand Reinhold, New York, 1950.
- [66] L. Schröter, S. Küchenhoff, R. David, W. Brening, H. Zacharias, *Surf. Sci.* 261 (1992) 243.
- [67] A. De Lange, E. Reinhold, W. Ubachs, *Int. Rev. Phys. Chem.* 21 (2002) 257.
- [68] J.B. Nelson, G.C. Tabisz, *Phys. Rev. Lett.* 48 (1983) 1393.